Basin Research (2008) **20**, 211–226, doi: 10.1111/j.1365-2117.2008.00354.x

Late Cretaceous to Miocene sea-level estimates from the New Jersey and Delaware coastal plain coreholes: an error analysis

M. A. Kominz,* J. V. Browning,† K. G. Miller,† P. J. Sugarman,‡ S. Mizintseva† and C. R. Scotese§

*Department of Geosciences, Western Michigan University, Kalamazoo, MI, USA
†Department of Geological Sciences, Rutgers University, Piscataway, NJ, USA
‡New Jersey Geological Survey, Trenton, NJ, USA
§Department of Geology, University of Texas at Arlington, Arlington, TX, USA

ABSTRACT

Sea level has been estimated for the last 108 million years through backstripping of corehole data from the New Jersey and Delaware Coastal Plains. Inherent errors due to this method of calculating sea level are discussed, including uncertainties in ages, depth of deposition and the model used for tectonic subsidence. Problems arising from the two-dimensional aspects of subsidence and response to sediment loads are also addressed. The rates and magnitudes of sea-level change are consistent with at least ephemeral ice sheets throughout the studied interval. Million-year sea-level cycles are, for the most part, consistent within the study area suggesting that they may be eustatic in origin. This conclusion is corroborated by correlation between sequence boundaries and unconformities in New Zealand. The resulting long-term curve suggests that sea level ranged from about 75–110 m in the Late Cretaceous, reached a maximum of about 150 m in the Early Eocene and fell to zero in the Miocene. The Late Cretaceous long-term (10^7 years) magnitude is about 100–150 m less than sea level predicted from ocean volume. This discrepancy can be reconciled by assuming that dynamic topography in New Jersey was driven by North America overriding the subducted Farallon plate. However, geodynamic models of this effect do not resolve the problem in that they require Eocene sea level to be significantly higher in the New Jersey region than the global average.

INTRODUCTION

Sea level is the datum against which vertical tectonics is measured, allowing scientists to better understand both Earth history and the response of the lithosphere and upper asthenosphere to stress (e.g. Burgess & Gurnis, 1995; Huismans *et al.*, 2001). Sea level is a significant control on sedimentation, generating stratigraphic packages that, in part, control the distribution of petroleum source and reservoir facies (e.g. Vail & Mitchum, 1977; Posamentier *et al.*, 1988) and groundwater resources (e.g. Sugarman *et al.*, 2005). Sea-level history also provides clues regarding the processes that generate global variations in the hydrosphere and lithosphere due to variations in ice (e.g. Fairbanks & Matthews, 1978; Camoin *et al.*, 2004) and ocean volumes (Pitman & Golovchenko, 1988; Harrison, 1990; Larson, 1991).

The difficulties of estimating past sea level are daunting (e.g. Miall, 1992). Proxies such as $\delta^{18}O$ are only sensitive to ice volume and do not include the various tectonic factors which change the volume of the ocean (e.g. Harrison, 1990). Additionally, $\delta^{18}O$ is dependent on other factors (e.g. temperature) and thus must be 'corrected' (e.g. Pekar *et al.*, 2002; Miller *et al.*, 2005a) in order to estimate sea level. Stratigraphic records are composed of tectonic, eustatic and sediment loading effects and thus, do not yield a direct estimate of sea-level change. This manuscript focuses on the assumptions made when removing tectonic and sediment loading from coastal plain coreholes collected from New Jersey and Delaware. It is important to recognize that stratigraphic data are subject to local and regional tectonic effects (e.g. Burgess & Gurnis, 1995; Hayden, 2008). Thus any sea-level record is local or regional, rather than eustatic (global). The eustatic estimate derived from backstripping New Jersey onshore coreholes (Van Sickel *et al.*, 2004; Miller *et al.*, 2005a) must be viewed in this context as a testable template against which other records can be compared. Expeditions designed to provide similar data sets from New Zealand and Australia will go far towards resolving the current sea-level curve into a valid eustatic estimate (e.g. Lu *et al.*, 2005). For now the previously reported eustatic curve derived from New Jersey backstripping (Van Sickel *et al.*, 2004; Miller *et al.*, 2005a) provides a testable model for comparison with other proxy

Correspondence: Michelle Kominz, Department of Geosciences, Western Michigan University, Kalamazoo, MI 49008, USA. E-mail: michelle.kominz@wmich.edu

datasets (e.g. oxygen isotopes). We present an update to the New Jersey backstripped estimates (Van Sickel *et al.*, 2004; Miller *et al.*, 2005a): (1) incorporating new data from more recently drilled coreholes (Ocean View, Sea Girt and Bethany Beach); (2) combining the datasets from different coreholes in a manner different from the previous averaging techniques; and (3) and providing a detailed error analysis.

GEOLOGICAL SETTING

The mid-Atlantic coast of North America is a passive continental margin that formed subsequent to Late Triassic to Early Jurassic rifting and volcanism (Steckler *et al.*, 1988; Benson, 2003). Tectonic evolution of a passive margin after the rifting stage is dominated by thermal cooling (McKenzie, 1978; Watts & Steckler, 1979; White & McKenzie, 1989). Coastal plain tectonics consists of early uplift due to heat transfer from the adjacent stretched and under-plated lithosphere, followed by subsidence due to sediment loading of the adjacent offshore basin (Steckler *et al.*, 1999). Thus, the subsidence phase of the coastal plain is tied to the offshore passive margin thermal subsidence. The magnitude of the coastal plain subsidence is a function of the rigidity of the plate and the thickness of the offshore sediment load. Thus, like the adjacent stretched margin, coastal plain subsidence follows the exponential decay of a cooling plate model (e.g. Stein & Stein, 1992). The simplest model of passive margin cooling is that of McKenzie (1978). Modifications of this model influence subsidence during the first tens of millions of years after rifting (Bond *et al.*, 1988). Because our data set does not include this period, we use a simple McKenzie (1978) plate model to estimate post-rift 'tectonic' subsidence of the coastal plain. Similarly, because our data do not include the first tens of millions of years after breakup, the uplift phase of the coastal plain is not included and only the subsiding portion of the coastal plain history is modelled.

The corehole data used in this manuscript are derived from an onshore drilling campaign that spanned onshore Ocean Drilling Program Legs 150X and 174AX (Browning *et al.*, 2005; Miller *et al.*, 1996, 1998, 1999b, 2003, Fig. 1). The most recent synopsis of the drilling results is reported in Browning *et al.* (2008). All drill sites examined here were drilled on land using an extended core barrel allowing 78–93% recovery. The coreholes were analysed to derive quantitative ages and palaeoenvironments. Ages, with resolution of about ± 0.5 m.y., are derived from strontium isotopes, biostratigraphy and limited magnetostratigraphy (Miller *et al.*, 1996, 1998, 1999b, 2003). Palaeoenvironments were obtained from evaluation of lithofacies and biofacies (Miller *et al.*, 1996, 1998, 1999b, 2003). Lithofacies were determined using sediment textures, structures and composition (including semi-quantitative counts for grain size, % glauconite, % coarse-fraction carbonate and % mica) integrated with downhole logs. Unconformities form the fundamental units dividing the stratigraphic record and were identified on the basis of physical stratigraphy, including irregular contacts, reworking, bioturbation, major facies changes, γ-ray peaks, and paraconformities inferred from biostratigraphic breaks. For the marine sections, benthic foraminiferal biofacies and lithofacies were used to infer palaeoenvironments. For the non-marine and nearshore sections (primarily the upper Miocene and younger section and mid-Cretaceous Magothy Formations), lithofacies interpretations provide the primary means of recognizing unconformities and interpreting palaeoenvironments.

Fig. 1. Location of coreholes used in this work. United States Geological Survey (USGS) wells used in the two-dimensional analysis and the projected cross-section of Kominz & Pekar (2001) are also shown.

BACKSTRIPPING METHOD

Backstripping removes the effect of the sediment load in order to determine how the basement would have subsided under water (*R*1, the first reduction of Bond *et al.*, 1989). This requires making assumptions about the compaction history of the sediments in order to estimate the sediment density (ρ_{S^*}) and sediment thickness (S^*) through time. In this paper, we use the porosity depth curves for sands and shales derived from New Jersey coastal plain coreholes

Table 1. Thermal Parameters for Ocean Subsidence

Ridge Parameters	Units	P&S*	S&S*	Ketal*
Depth ridge	meters	2500	3178	2960
Thickness plate	km	125	95	92.5
Diffusivity	cm^2/s	31.56	25.2	17
Coefficient of expansion	/°K	3.28×10^{-05}	3.10×10^{-05}	3.10×10^{-05}
Temperature – Asthenosphere	°C	1350	1450	1450
Specific heat	cal/g/°K	0.28	0.28	0.28
Conductivity	cal/°K/cm/s	0.0075	0.0075	0.0075
Thermal decay constant	m.y.	62.8	36	62

*P&S is Parsons & Sclater (1977). S&S is Stein & Stein (1992) and the thermal parameter that we use (Ketal) are based on our own analysis of age vs. depth data in which only plate thickness and thermal diffusivity were changed to fit the relationship observed from 2.4 million 0.1 × 0.1 degree world oceans grid points (Kominz & Scotese, 2005).

by Van Sickel *et al.* (2004). If the data set is distributed in two or three dimensions, then it is possible to take into account the lateral strength of the lithosphere (Φ) (Steckler & Watts, 1978; Steckler *et al.*, 1999; Kominz & Pekar, 2001). The sediment and sea-level (ΔSL) loads are compensated flexurally (Φ) or one-dimensionally (Φ = 1) by the asthenosphere (density of ρ_a). The palaeo-water depth, (WD) is a direct contribution to *R*1. Finally, *R*1 is calculated using the following equation:

$$R1 = \Phi\left[S^*\left(\frac{\rho_a - \rho_{S^*}}{\rho_a - \rho_w}\right)\right] + \mathrm{WD} = \mathrm{TS} + \Delta\mathrm{SL}\left(\frac{\rho_a}{\rho_a - \rho_w}\right) \quad (1)$$

*R*1 in this equation is the depth to the basement in water, which is a combination of tectonic subsidence (TS) and sea-level change. As discussed above, for the Mid-Atlantic coastal plain, TS follows the form of a thermally cooling plate. Thus, TS is estimated by fitting a cooling plate model to *R*1. The difference between *R*1 and TS is used to calculate *R*2 [the second reduction of Bond *et al.* (1989)], which, in the absence of tectonics is sea-level change (ΔSL):

$$\Delta SL = \left(\Phi\left[S^*\left(\frac{\rho_a - \rho_{S^*}}{\rho_a - \rho_w}\right)\right] + \mathrm{WD} - \mathrm{TS}\right)\left(\frac{\rho_a - \rho_w}{\rho_a}\right) \quad (2)$$

$$R2 = \Delta\mathrm{SL} = (R1 - \mathrm{TS})\left(\frac{\rho_a - \rho_w}{\rho_a}\right) \quad (3)$$

Cooling Plate Model

As discussed above, accommodation is generated beneath the coastal plain of the central US Atlantic margin according to a cooling plate model in response to the stretched and underplated continental margin (Steckler *et al.*, 1988; White & McKenzie, 1989). The form of the cooling plate is dominantly exponential (after about 10 Ma)

$$\text{Depth sea floor} = \text{depth old sea floor} - \text{slope} \times e^{-\text{time}/\text{decay constant}} \quad (4)$$

The decay constant is obtained from the age vs. depth relation of the ocean floor, which is taken to be the end member, or fully stretched continental lithosphere (McKenzie, 1978). Several estimates of the age–depth relation of the ocean have been made using various thermal parameters (Table 1).

Our model for ocean floor subsidence (subsequently termed Ketal) was derived using recent digitized sea floor age data, depth data and sediment thickness data (Müller *et al.*, 1997; Smith & Sandwell, 1997; Divins, 2006). It is similar to that of Parsons & Sclater (1977) and results in a flatter thermal decay curve than that of Stein and Stein (1992). This, in turn, results in a somewhat greater magnitude of long-term sea-level change when considering the difference between *R*1 and theoretical TS.

The Millville corehole results are presented as an example of this method in Fig. 2. The sea-level estimate made from taking the difference between the calculated subsidence, *R*1, and thermal subsidence is dependent on the thermal parameters used to calculate plate cooling. The magnitude of sea-level change is made by comparison with the current elevation of the Millville corehole, which is 27.3 m above sea level.

The Millville corehole includes sediments ranging from uppermost Lower Cretaceous to the Holocene. As is the case for all of the coreholes, sediment has been included beneath the corehole to take into account the compaction of the sediment below the corehole and above basement. Deposition of sediment beneath the Millville corehole was assumed to have occurred between 120 and 97 Ma and thicknesses were estimated from seismic reflection data (Sheridan *et al.*, 1991). This portion of the curve is not included in sea-level estimates due to the lack of detailed lithology, age and water depth data. However, as Fig. 2 shows, the early subsidence history plays a significant role in the shape of the long-term sea-level curve de-

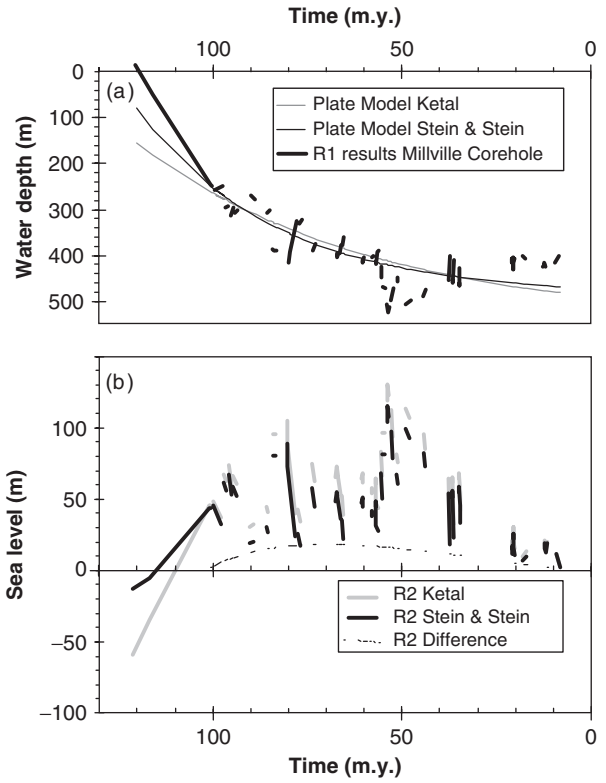

Fig. 2. (a) *R*1 subsidence for Millville corehole. Millville *R*1 data are fit to two theoretical thermal curves based on the Stein and Stein model (1992; S&S) with a thermal decay constant of 36 Myr and our model (Ketal) with a thermal decay constant of 62 m.y. (b) The difference between the theoretical plate model subsidence and the observed *R*1 data, after correction for water loading [Eqn (3)]. Also shown is the difference between the two *R*2 results, which is equal to the difference between the two theoretical curves (S & S and Ketal) in (a).

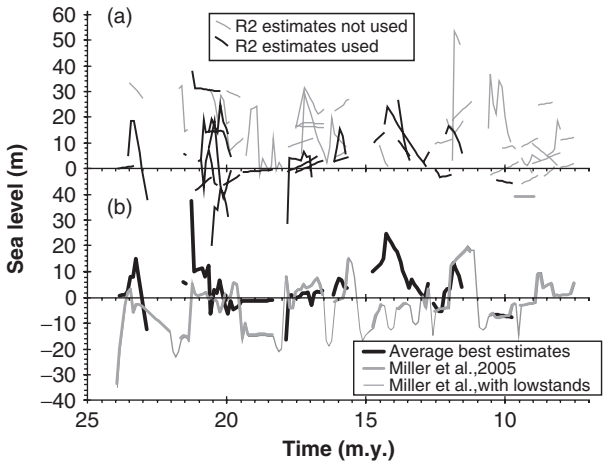

Fig. 3. (a) All Miocene *R*2 curves for all coreholes are plotted in grey and black. Of these, only the black curves have sufficient age and water depth control for inclusion in our sea-level curve. (b) The black thick curve shows the averages of the *R*2 estimates that have good age and water depth constraints from (a). The thick grey curve includes all sequences analysed and modelled by Miller *et al.* (2005a). The thin grey line connecting these sea level estimates indicates that between sequences sea level was assumed to have been relatively low.

rived from the later history. Thicker underlying sediments result in a greater misfit to the theoretical curve at early ages. This uncertainty diminishes to zero at the top of the core. The age at which deposition begins has a similar, minor, impact on the long-term sea-level trend. That is, as the assumed age of initiation of subsidence is made younger, the Cretaceous sea level gets slightly higher. In this case, the maximum increase in sea level is about 1.3 m for a reduction in age of the initiation of sedimentation from 120 to 110 Ma. Finally, the timing of initiation of thermal subsidence has an effect on the thermal curve, and thus, the predicted *R*2 values. In the case of Miller *et al.* (2005a) and Van Sickel *et al.* (2004), we used the timing of initial subsidence below sea level of each well and not the timing at which thermal subsidence began in the stretched margin. Here, we use the breakup age of 175 Ma for the initiation of thermal subsidence. The result is a flatter thermal plate model and an increase in *R*2 by <2 m with the largest effect occurring in the Late Cretaceous and decreasing to near zero in the Miocene.

The impact on the long-term sea-level curve of the thermal parameters used to estimate 'TS' is not insignificant. The maximum difference in the sea-level estimates made from fitting the two different ocean floor models is about 17 m and occurs at about the K/T boundary. The two data sets are both fixed to the same values near the present (in the case of Millville, 27.3 m above present sea level) and the two thermal models are identical at about 20 and 90 Ma (Fig. 2a). Thus, it is reasonable that the maximum difference should occur at about 65 Ma, near the centre of the data set (Fig. 2b). The sea-level estimates of Miller *et al.* (2005a) were made by fitting the *R*1 curves to the Stein & Stein (1992) ocean ridge model. In this manuscript, we use the Ketal parameters that again yield a higher long-term Cretaceous sea-level estimate.

Ages and Water Depths

The age data available for the Middle Atlantic coastal plain coreholes are derived from integrated biostratigraphy and strontium isotope stratigraphy that provide excellent age control (better than 1 m.y. resolution, with finer resolution in intervals with magnetostratigraphy). Despite this, there are age uncertainties that were resolved using stratigraphic paradigms. For example, more deeply buried strata were always taken to be older than shallower strata. Additionally, the sequence stratigraphic model (e.g. Posamentier *et al.*, 1988) was used, in that the ages below an unconformity were taken to be older than those above an unconformity (e.g. Pekar *et al.*, 2000). Finally, where age data were lacking, strata were correlated to dated strata in other coreholes. This was particularly the case for the Miocene sequences used in Miller *et al.* (2005a). Here, we include only the Miocene sequences which have well-constrained dates and water depths in our sea-level estimates. Figure 3a shows all Miocene age *R*2 estimates with only best-estimate water depths, [WD in Eqn. (2)] assumed. Less than half of these are sufficiently well dated to be used to calculate sea level.

The average of those curves is compared to the Miller *et al.* (2005a) estimates in Fig. 3b. The two curves are significantly different and that difference is mainly a result of leaving out the poorly constrained sequences.

One clear limitation of backstripping coastal plain sequences to estimate the magnitude of sea level is the fact that sea-level lowstands are not recorded on the coastal plain. This is indicated by the gaps in the *R*2 curves (e.g. Figs 2 and 3) that correspond to unconformities at the coastal plain. Thus, it is impossible to obtain the full magnitude of sea-level changes in this setting. Miller *et al.* (2005a) generated a curve which included sea-level falls associated with all sequence boundaries (Fig. 3b). This thin curve is not meant to indicate that the magnitude of the fall is known, but rather to focus awareness on the assumption that sea level was lower during hiatuses. There are a few exceptions in the Cretaceous that sampled lowstand deposits and thus, sample a fuller, if not complete, range of sea level.

Assuming that *R*2 is actually an indicator of sea level, one might expect that both the timing and the amplitude of *R*2 should be the same for all correlative sequences, or at least for those that are well constrained (black *R*2 values in Fig. 3a). We find that the timing of these sequences are quite similar, although their amplitudes often are not. Part of the reason for the amplitude discrepancy is the fact that we have only plotted 'best estimate' water depths. Our water depth estimates are based on a combination of benthic biofacies and physical indicators. These cannot yield precise, quantitative palaeo water depths, but rather, produce a range. Thus, a better test for the validity of these *R*2 estimates as sea-level indicators is whether or not the range of *R*2 values overlaps for correlative coreholes.

To show the range of results when palaeowater depth ranges are taken into account, we focus on the three youngest Miocene sequences that are well dated with relatively precise water depth estimates and ranges (Fig. 4). The Kw-Ch3 sequence is well constrained only at the Cape May corehole. As a result, the water depth range at Cape May generates the full range of uncertainty in *R*2. Sequence Kw3 is represented and well dated in three coreholes, Cape May, Ocean View and Atlantic City. In this case, all three *R*2 curves overlap. As such, the overlap of all error ranges yields the range of *R*2 values that are consistent with all three coreholes. Thus, the range of *R*2 is taken to be all *R*2 values between the minimum high-end estimate and the maximum low-end estimate (Fig. 4b), that is, the range of overlapping *R*2 results. Where the sequences overlap (Kw3), the minimum high-end estimate forms the upper error range. This is found at Atlantic City at 13.8 Ma and shifts to Cape May at 13.5 Ma. The maximum low-end error bar begins as Cape May at 13.8 Ma and shifts to Ocean View at 13.6 Ma. The most problematic result is the case where the *R*2 estimates for sequences observed at two or more boreholes do not overlap. That is, the *R*2 results are inconsistent with a simple sea-level interpretation. An example is sequence Kw-Ch1, which is present at both the Ocean View and the Cape May coreholes.

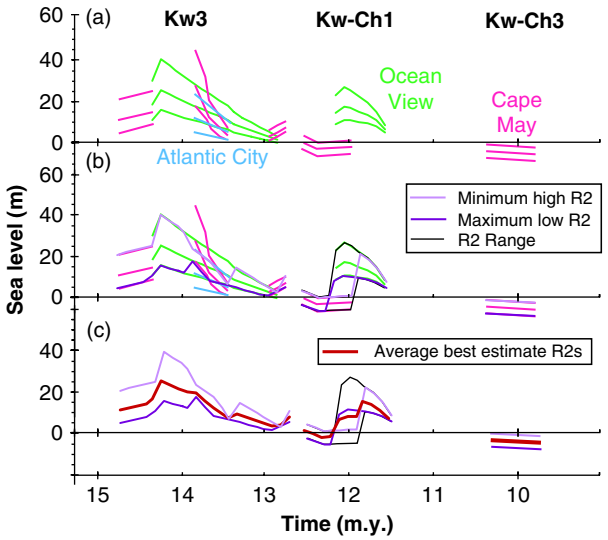

Fig. 4. (a) Three youngest Miocene sequences used in our analyses with error ranges of sequences. (b) The same sequences with superimposed lowest maximum value (light purple line), highest minimum value (dark purple line). Where two or more sequences do not have overlapping ranges (e.g. sequence Kw-Ch1) the maximum range of *R*2 values are used (black lines). (c) One-dimensional *R*2 error ranges and averages based on the data shown in (a) and their relationships shown in (b). The light purple line is the lowest maximum value, the red line is the average of the best estimates and the dark purple line is the maximum low estimate for each 0.1 m.y. interval. The maximum range of *R*2 (black line) is used where sequences that occur at the same time do not yield overlapping *R*2 estimates.

Where the two coreholes overlap in time, the minimum estimate of *R*2 from Ocean View is higher than the maximum estimate of *R*2 from Cape May. This can also be observed as the maximum low estimate being higher than the minimum high *R*2 estimate. In this case, we use the maximum range of uncertainty obtained from all boreholes as our sea-level range (Fig. 4b and c).

Also plotted with the error ranges on *R*2 are the averages of the best-estimate *R*2 values (Fig. 4c). This is the method used to estimate sea level by Miller *et al.* (2005a). In most cases the average values fall between the minimum ranges. These values are not expected to fall on the mid-point between the minimum *R*2 ranges for several reasons. First, the 'best estimate' water depth values are not expected to be mid-way between the high and low water depth estimates. In general, the biofacies analysis and facies descriptions provide 'best estimate' water depths. However, both methods are imprecise and the uncertainty increases with depth. In order to take into account these uncertainties a minimum water depth is assigned that is 60% of the best estimate and a maximum water depth is assigned that is 150% of the best estimate. This results in a low estimate that is closer to the 'best estimate' than the high end, consistent with the fact that the habitat ranges of benthic fauna (used to estimate water depth) broaden with increasing depth. Thus, the best estimate is not the mean of the ranges. Second, the *R*2 curves are not a direct measure of

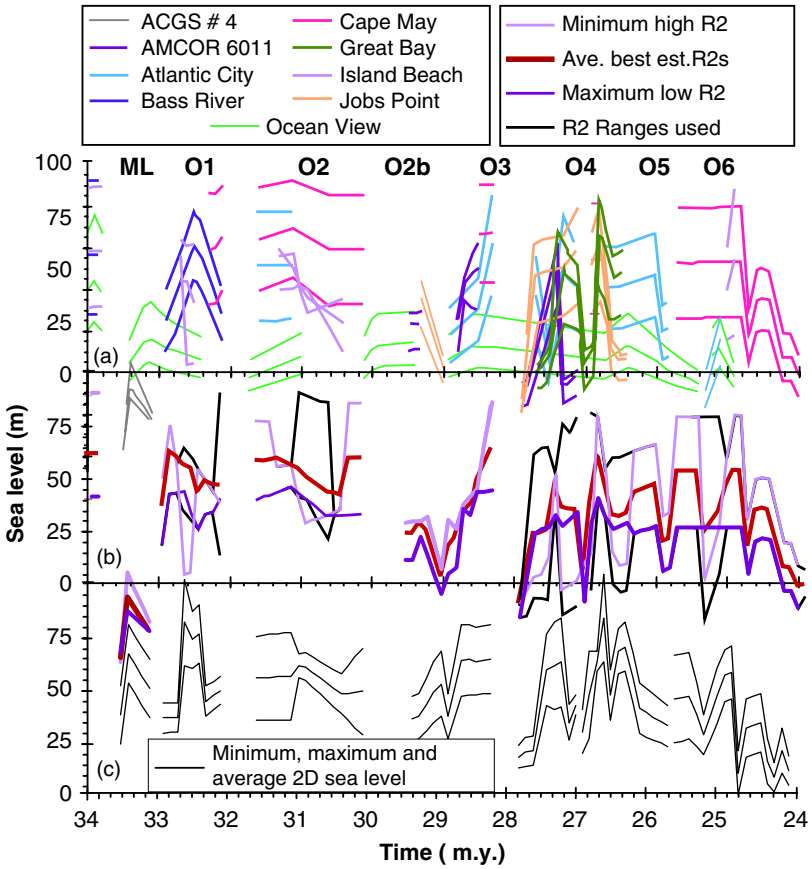

Fig. 5. (a) One-dimensional *R*2 results from nine Oligocene coreholes. The thin green line shows the Ocean View *R*2 results that were not included in the two-dimensional (2D) backstripping (Kominz & Pekar, 2001) and are not included in the averages and ranges of (b). (b) One-dimensional *R*2 error ranges and averages based on the eight coreholes that were used in the 2D analysis. The light purple line is the lowest maximum value, the red line is the average of the best estimates and the dark purple line is the maximum low estimate for each 0.1 m.y. interval. Black lines give the full range of *R*2 results when two or more sequences that occur at the same time do not overlap in magnitude. (c) The minimum, maximum and best-estimate sea-level curves from Kominz & Pekar (2001). These were estimated using a 2D backstripping approach.

the water depth differences because each *R*1 curve (based on the low WD, the best-estimate WD and the high WD) is fit to a thermally cooling plate model and *R*2 is the difference between each *R*1 curve and it's best-fit thermal model (see e.g. Fig. 2). Finally, the averages of the best estimates are based on all overlapping sequences whereas the maximum and minimum ranges are only based on the two sequences that generated them: that is, the minimum high and maximum low estimates (if results are internally consistent) or the absolute maximum and minimum estimates (if results are internally inconsistent). Thus, where more than two sequences are observed at any given time, the average of the best estimates is not expected to parallel the ranges, as is seen for sequence Kw3. In fact the average *R*2s need not even fall between the ranges. The fact that they do, suggests our assumption that *R*2 is dominantly a sea-level signal may be true.

Two-Dimensional (2D) Sequences and Flexural Response to Sediment Loads

One source of error in our sea-level estimates stems from the fact that the sedimentary sequences that were deposited in this environment in response to sea level, tectonics and local sediment supply form a 3D geometry (e.g. Greenlee & Moore, 1988; Fulthorpe & Austin, 1998). As such, water depths (and ranges of water depth estimates) for deposits of the same age must vary from corehole to corehole. Additionally, the response of the lithosphere to the sediment load was flexural, [$\Phi \neq 1$ in Eqns (1) and (2)]. We can begin to consider the impact of ignoring these 3D considerations on our 1D model by comparing our 1D model with the 2D backstripping of the Oligocene section in this region by Kominz & Pekar (2001).

The Kominz & Pekar (2001) 2D backstripping approach has its own sources of error, not the least is the fact that they took a 2D approach to a 3D problem. A limited number of wells (ACGS#4, Bass River, Island Beach, AMCOR 6011, Jobs Point, Great Bay, Atlantic City, and Cape May) were projected into a single 3D cross-section (Fig. 1). Thus, lateral variability in deposition was either erroneously introduced into the model or eliminated entirely. The resulting self-consistent sequence model (Pekar *et al.*, 2000) and the internally consistent 2D backstripping results (Kominz & Pekar, 2001) suggest that the 2D approach was reasonable for this time interval and it is impossible, at present, to assess any errors introduced by it.

The overall timing and shape of the averaged sea-level estimates from this work and the best estimates from 2D backstripping are quite similar (compare Fig. 5b and c). One detail that is lost in the averaging method is short sequence boundaries. In order to compare sequences, they have been interpolated into 0.1 m.y. increments. Where a sequence boundary is 0.1 m.y or less in duration, the averaging of the 1D *R*1 curves does not distinguish the presence of an unconformity, which is below the resolution of our data. Thus, sequences O4, O5 and O6 are not separated by the 1D approach. Similarly, high-frequency varia-

tions (100 k.y. or shorter period variability, as in many Milankovitch scale periods) are below the resolution of this method.

In some cases, 1D analyses result in an error in the overall magnitude of a sequence, with respect to other sequences by as much as 40 m (sequence ML, Fig. 5b and c). Using the 2D approach it was possible to precisely model the lateral and vertical relationships between deposition at each well. Without these relationships, vertical changes in deposition may be mistaken for vertical changes in sea level. For example, the inconsistent results of sequences O2, O4, O5 and O6 are all resolved by using the 2D approach.

There are many differences in detail between the average 1D and the 2D best estimates. There are two advantages of the 2D approach that generate these differences. First, again, the vertical and horizontal relationships between all coreholes are modelled. Second, many of the *R*2 estimates from individual coreholes are often based on interpolation between well-defined water-depth estimates. For the 2D model, only the locations with benthic biofacies-derived water-depth estimates were used to generate the sea-level curve. That is, using a 2D approach, it was possible to use the individual samples within a sequence, which had both age and depth control to estimate sea-level change. Thus, the 2D results of Kominz & Pekar (2001) are taken to represent the best estimate of sea level for the Oligocene and are used in our final sea-level curve.

It is worth noting that the Ocean View sequences yield *R*2 values, which overlap those of the eight wells used in the 2D analysis. However, the timing of the sequences is quite different from that of the other eight coreholes that sampled Oligocene strata. Because the Ocean View sequences have not yet been integrated into either the 2D sequence stratigraphic model or the benthic biofacies model of Pekar *et al.* (2003), it is difficult to make a valid comparison and Ocean View is not used in constructing the Oligocene sea-level curve in this paper.

The error ranges obtained by utilizing the lowest maximum and highest minimum estimates from the 1D *R*2 curves are generally, but not always as large or larger than those obtained with the 2D approach. Use of the total range of results where individual wells do not overlap results in larger error bars than the 2D results (Fig. 5b). In cases where sequences present at multiple coreholes overlap (error ranges do not cross in Fig. 5b) the overall form of the curves and the error ranges obtained from the 1D approach are quite similar to those obtained from the 2D approach. Where two or more *R*2 results do not overlap, the results are more problematic. In fact, there are times (32.1 Ma in sequence O1, 31.0–30.6 Ma in sequence O2; 27.8–27.5 and 27.3–27.1 Ma in sequence O4, 26.9 and 26.6–26.4 in sequence O5 and 25.3–25.1 Ma in sequence O6) in which the average best estimates fall outside of these ranges. In these cases use of the maximum error range for all sequences results in much broader error range than that obtained using the 2D approach.

Comparing the 1D and 2D results provides the impetus for the method used in this manuscript to generate a sea-level curve from 1D data, which is applied to the entire record, except the Oligocene. Therefore, the upper bound of the range of sea levels in the sea-level curve, we generate in this work's maximum range is the maximum value of either: (1) the lowest high-end *R*2 value where all overlapping sequences are consistent; (2) the highest *R*2 estimate where overlapping sequences yield inconsistent results; or (3) the average best estimate result if it is higher than the above. The lower bound of the range of sea levels in our curve is the minimum value of either: (1) the highest low-end *R*2 value where overlapping sequences yield consistent results; (2) the lowest *R*2 value where overlapping sequences yield inconsistent results or; (3) the average of the best estimates if that is less than these two results. Our best-estimate curve is the average of the best estimates.

RESULTS: THE SEA-LEVEL CURVE

The overall sea-level curve is quite similar in form to that which we previously published (Fig. 6, Miller *et al.*, 2005a). Miocene sea level was quite low and the amplitudes of the signals recorded at the coastal plain sites were also generally low in both compilations. The highest sea levels occurred in the early to middle Eocene. However, in the new

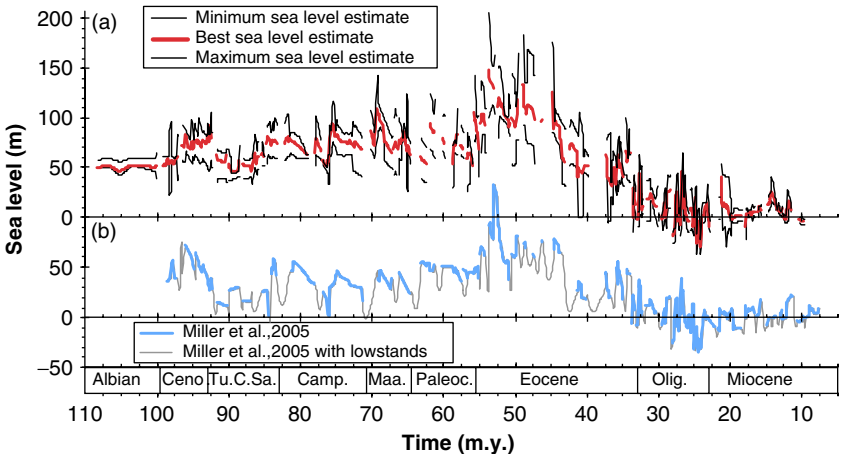

Fig. 6. (a) One-dimensional *R*2 estimates, including error ranges. (b) One-dimensional *R*2 results of Miller *et al.* (2005a). (Ceno., Cenomanian; Tu.C.Sa, combined Turonian, Coniacian and Santonian; Camp., Campanian; Maa., Maastrichtian; Palaeoc., Palaeocene; Olig., Oligocene).

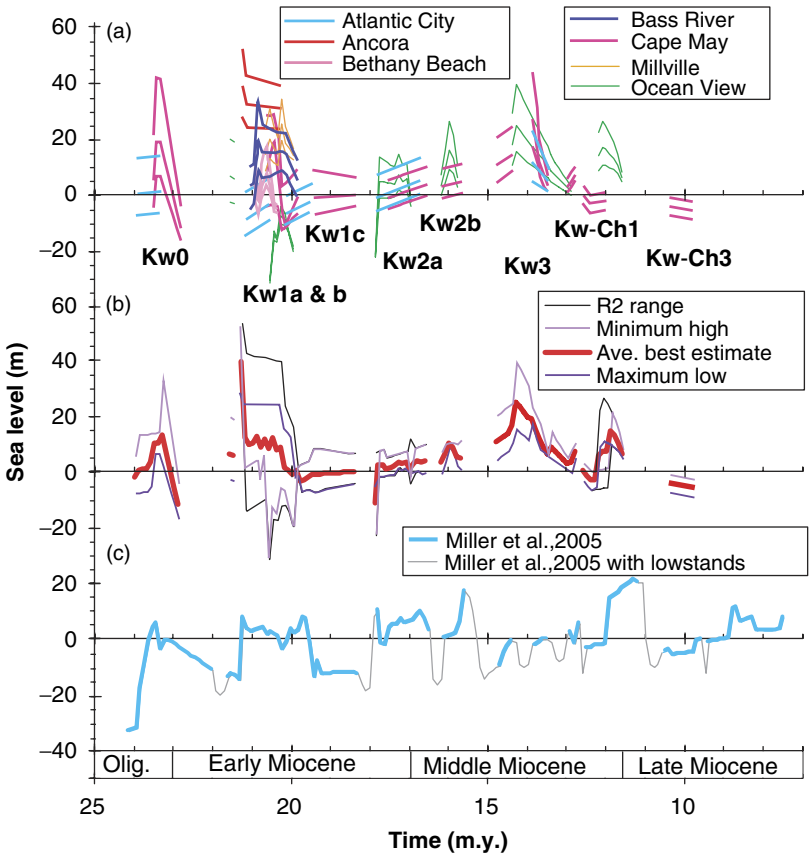

Fig. 7. (a) One-dimensional Miocene *R*2 curves from Cape May, Island Beach, Atlantic City, Bass River, Ancora, Millville and Bethany Beach coreholes. (b) Minimum high-*R*2, maximum low-*R*2 and averaged best estimate *R*2 results. Black lines give the full range of *R*2 results when two or more sequences that occur at the same time do not overlap in magnitude. (c) *R*2 best estimate averages from Miller *et al.* (2005a). (Olig., Oligocene).

compilation, the sea-level high was broadly distributed over several sequences and 5–10 m.y. rather than occurring as a single sequence in our earlier work. The Cretaceous sequences in both compilations exhibit high amplitude fluctuations (as much as 15–40 m in <1 m.y.), consistent with the presence of small, land-locked ice sheets (e.g. Miller *et al.*, 1999a, 2005a). Additionally, the overall amplitude of the long-term Cretaceous sea-level signal is higher than our earlier work. This is largely a result of the thermal properties assumed for subsidence of the lithosphere and, to a lesser extent, the timing of thermal subsidence initiation. In the following section, we provide a detailed comparison of the new curve with our earlier results and the *R*2 data on which the new curve is based.

Miocene *R*2 Results

The Miocene sea-level curve from this work is actually quite different from that of Miller *et al.* (2005a, Fig. 7b and c). As discussed above, this is a result of removal of sequences in which either the ages or the environments were poorly constrained and addition of new sequences from coreholes that had not been analysed 3 years ago (of these, Ocean View, Bethany Beach and Millville contain Miocene strata). It is important to note that a sea-level fall is seen between 12 and 10.5 m.y. (Kw-Ch1 to Kw-Ch3 in Fig. 7) corresponding with that measured at 56 ± 11.5 m at the Marion Plateau by John *et al.* (2004). We see only 23 ± 13 m of sea-level fall. However, our data set does not capture the lowstand, which could include the missing 10–57 m of sea-level fall. The Ocean View corehole yielded a single sequence, Kw3 spanning the time period previously separated into three small sequences. By incorporating results from Ocean View, Cape May and the Atlantic City coreholes the multiple rise and fall aspect of this time period is maintained whereas the nondepositional periods between sequences are eliminated. The Ocean View results have modified the remainder of the Miocene sequences, although not as intensely as during deposition of sequence Kw3.

The Oligocene sequence is taken to be that of the 2D model of Kominz & Pekar (2001). This was also true of Miller *et al.* (2005a) and has been discussed in detail above.

Eocene *R*2 Results

The Eocene *R*2 data have been expanded relative to Miller *et al.* (2005a) by the addition of the Ocean View, Millville and Sea Girt coreholes (Fig. 8a). The Eocene results are quite consistent among the seven coreholes so that in most cases the *R*2 results are overlapping for the 11 Eocene sequences. That is, the lowest high-*R*2 estimate is above the highest low-*R*2 estimate (Fig 8a and b). This suggests a robust Eocene sea-level signal. The biggest change in the Eocene section is the removal of the sea-level maximum at 53 Ma (Fig 8b and c). This occurred due to revision of the dates used for the Ancora *R*2 curves in Miller *et al.* (2005a). The *E*2 sequence had been shifted into the period between *E*2 and *E*3. The maximum sea-level estimate from the New Jersey Coastal Plain now occurs in sequence *E*2 at about 53.5 Ma (Fig. 8b). The magnitude is about 140 m

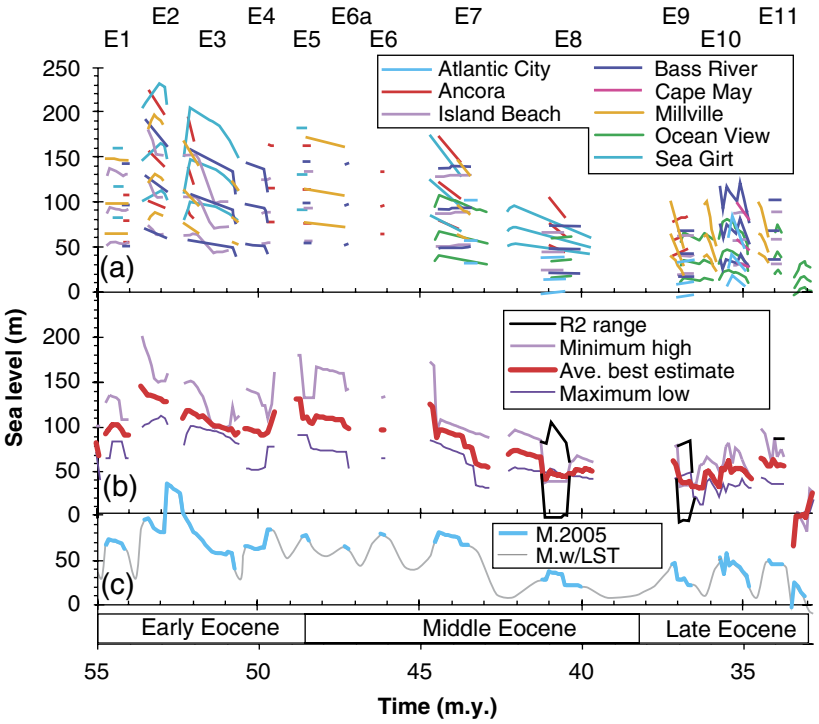

Fig. 8. (a) One-dimensional, Eocene *R2* curves from Cape May, Island Beach, Atlantic City, Bass River, Ancora, Millville, Ocean View and Sea Girt coreholes. (b) Minimum high-*R2*, maximum low-*R2* and averaged best estimate *R2* results. Black lines give the full range of *R2* results when two or more sequences that occur at the same time do not overlap in magnitude. (c) *R2* best estimate averages from Miller *et al.* (2005a). (M. 2005, Miller *et al.* (2005a); M. w/LST, Miller *et al.* (2005a) with conceptual lowstands included).

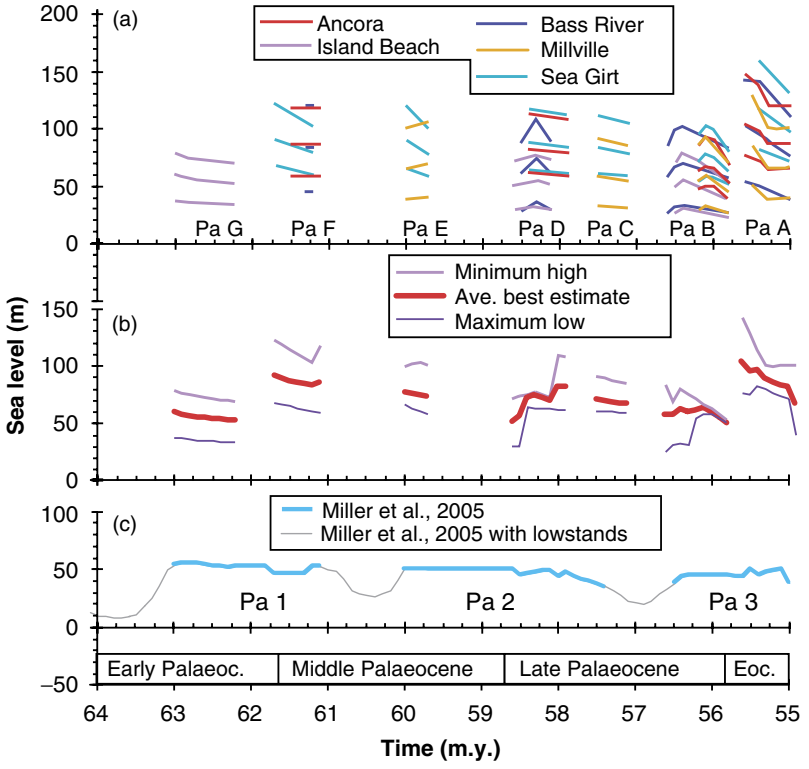

Fig. 9. (a) One-dimensional Palaeocene *R2* curves from Island Beach, Bass River, Ancora, Millville, and Sea Girt coreholes. Sequence PaA is included with the Palaeocene sequences because it had been part of Pa3, which overlaps the Eocene and Palaeocene (c). (b) Minimum high-*R2*, maximum low-*R2* and averaged best estimate *R2* results. (c) *R2* best estimate averages from Miller *et al.* (2005a). (Eoc., Early Eocene).

above present sea level, about the same as the previous, slightly younger peak of Miller *et al* (2005a) of 132 m.

Palaeocene *R2* Results

The Palaeocene *R2* results are even more impressive than those of the Eocene in that the *R2* estimates generated at the five coreholes are not only internally consistent, but improved dating has resulted in the definition of seven sequences where we previously could only identify three sequences (Fig. 9). Dating is based primarily on calcareous nannoplankton and secondarily on foraminifera, whereas water depths were based dominantly on the distribution of benthic foraminifera. In this coastal plain setting, we

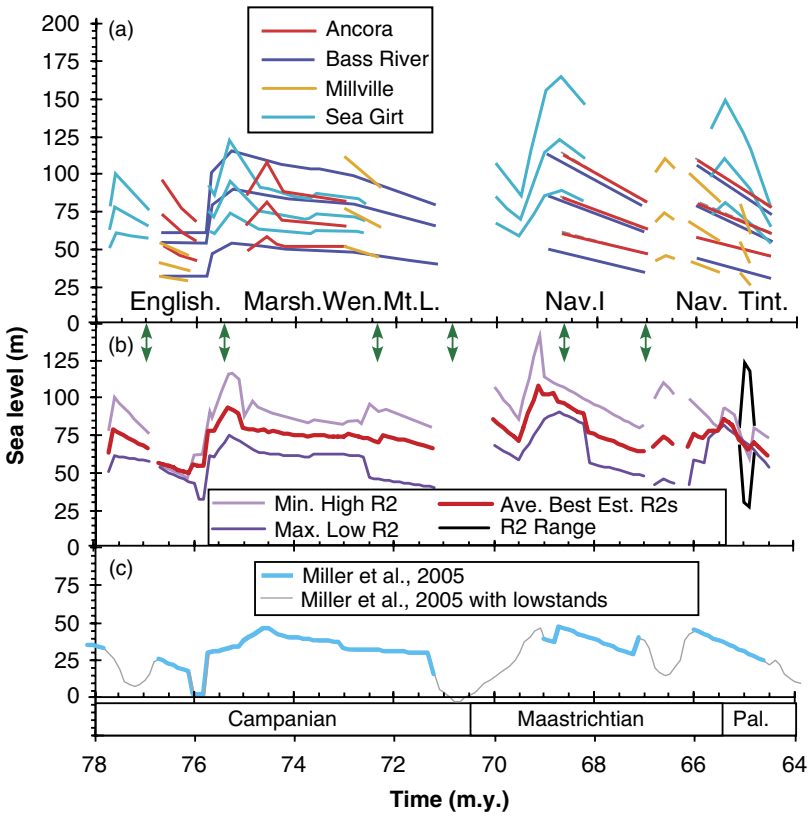

Fig. 10. (a) One-dimensional Maastrichtian and Campanian *R2* curves from Bass River, Ancora, Millville and Sea Girt coreholes. (English., Englishtown Formation; Marsh.Wen.Mt.L., Marshalltown, Wenonah and Mount Laural Formations; Nav.I., Navesink and New Egypt Formations; Tint., Tinton Formation). The earliest Palaeocene (Pal.) is included in this plot because the Navesink Formation overlaps the Cretaceous–Tertiary boundary. Green double-headed arrows show the timing of major unconformities in New Zealand (Crampton *et al.*, 2006). (b) Minimum high-*R2*, maximum low-*R2* and averaged best estimate *R2* results. Black lines give the full range of *R2* results when two or more sequences that occur at the same time do not overlap in magnitude. (c) *R2* best estimate averages from Miller *et al.* (2005a).

expect that only the highstand portion of sea level will be recorded, with unconformities and non-deposition marking the periods in which sea level was not high enough to cover the coastal plain. Overall, the *R2* results suggest that sea level was 25–125 m above present with some variability. This is about 25 m or so above and considerably more variable than the Miller *et al* (2005a) Palaeocene sea-level estimates, which were quite constant at about 25–60 m above present sea level.

Cretaceous *R2* Results

Calculations of Cretaceous sea level include results from three new coreholes (Millville, Sea Girt and Fort Mott). These have been added to the previous results from the Bass River and Ancora coreholes (Figs 10 and 11). The Late Cretaceous *R2* values are almost entirely internally consistent, because they overlap in both magnitude and timing, suggesting that we are looking at a sea-level-dominated signal. In some cases, the new sequences seem to eliminate sequence boundaries. For example, the three Bass River, and the Merchantville I and II sequences, are no longer discernable as separate sequences. This is because the sequence boundary has a duration of 0.1 m.y., which is our interpolation interval. Thus, although it is likely that sea level was lower during that interval, it is below the resolution of this study and the sequences appear to be uninterrupted. In other cases there appears to be overlap between the timing of deposition of sequences at different coreholes. This is particularly the case for the Englishtown and Marshalltown through Mount Laural formations observed at the Bass River corehole. The age control of these sequences is relatively poor and this is the source of the inconsistent timing of deposition between locations. The variations could also reflect a 3D response to loading from sediment in combination with sea-level change (e.g. Pekar *et al.*, 2000; Posamentier *et al.*, 1988) that cannot be confirmed through 1D modeling.

The Cretaceous *R2* results are consistent with those predicted by Miller *et al.* (2005a, Figs 10 and 11). The long-term (10^7-year scale) highstand of sea level was about 75–100 m above present sea level, which is about 20–60 m above the Miller *et al.* (2005a) estimates. This discrepancy is largely due to the details of the thermal model used to estimate TS as described above. That is, we assume thermal parameters consistent with ocean floor subsidence with an exponential decay constant of 62 rather than 36 m.y. yielding a flatter thermal curve and higher Cretaceous *R2* values (Table 1 and Fig. 2). The assumption that thermal cooling began at about 175 Ma, about 50 m.y. earlier than Miller *et al.* (2005a), also raised these values by a few metres, as discussed above.

Sequences studied here have a 0.5–3 m.y. duration and are thus equivalent to both the second and third-order sequences of Exxon Production Research Company (EPR, Vail and Mitchum, 1977; Haq *et al.*, 1987). The amplitudes of sea-level variations observed on this scale are consistent with those of Miller *et al.* (2005a) and Van Sickel *et al.* (2004) but are exceeded by the EPR estimates by a factor of two to three. Variations in best estimate sea level remain <40 m within and between sequences, although the uncertainty could result in variations of as much as 75 m of sea-level

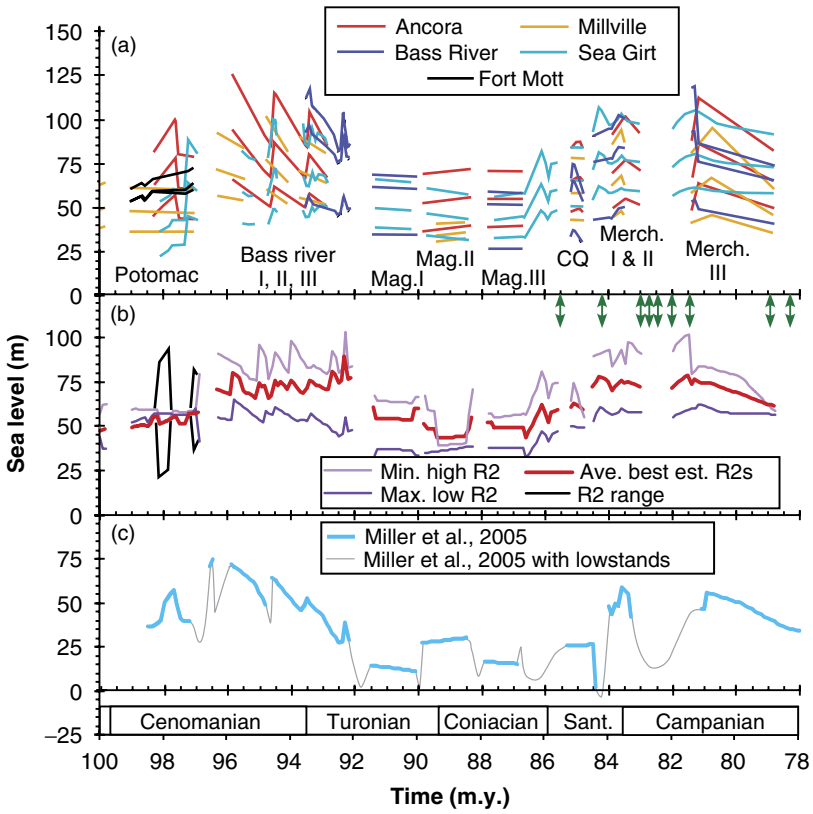

Fig. 11. (a) One-dimensional Cenomanian through earliest Campanian *R2* curves from Bass River, Ancora, Millville, Sea Girt and Fort Mott coreholes. Green double-headed arrows show the timing of major unconformities in New Zealand (Crampton *et al.*, 2006). (Mag., Magothy Formation; CQ, Cheesequake Formation; Merch., Merchantville Formation; Merchantville III includes the Woodbury and lower Englishtown Formations.) (b) Minimum high *R2*, maximum low *R2* and averaged best estimate *R2* results. Black lines give the full-range of *R2* results when two or more sequences that occur at the same time do not overlap in magnitude. (c) *R2* best estimate averages from Miller *et al.* (2005a). (Sant. = Santonian).

change (Figs 10 and 11). The required sea-level changes are sufficiently large and rapid to require the formation and removal of small ice caps (e.g. 69, 75.5 and 92 Ma, Figs 10 and 11; Miller *et al.*, 2005b). Recent isotopic evidence of a small ice cap 91 Ma (Bornemann *et al.*, 2008) may be associated with the sequence boundary between the Magothy I and II sequences or between the Magothy I and Bass River III sequences.

Crampton *et al.* (2006) estimated the timing of basin-wide unconformities in the East Coast Basin of north-central New Zealand. Although their timescale is not precise, they found a strong correlation of eight of their unconformities with the sequence boundaries of Miller *et al.* (2005a), suggesting that the events are eustatic. Eleven of the New Zealand unconformities correspond with sequence boundaries in our new sea-level curve (Fig 10 and 11). These include unconformities at 67, 71, 77, 84 and 85.5 Ma as well as four unconformities that correspond to a large gap in the New Jersey record between the Merchantville II and III sequences (Fig 11 and 12). However, a second unconformity falls in the middle of the Navesink I sequence (Fig 10). Additionally, two of the New Zealand unconformities (75.5 and 81.5 Ma) are closely associated with significant sea-level falls in New Jersey (Figs 10 and 11). Two New Zealand unconformities (72.5 and 68.7 Ma) are not associated sequence boundaries in New Jersey (Fig 10). As suggested by Crampton *et al.* (2006) the fact that 10–11 of the 15 New Zealand unconformities match New Jersey sequence boundaries and two are associated with sea level falls is a strong indication that this signal is eustatic in origin.

Comparison with other long-term estimates of sea-level change

Our revised estimates for the Late Cretaceous peak sea level of ~75–110 m is in reasonable agreement with the best estimate of 100 ± 50 m of Miller *et al.* (2005a) derived from various sources. Miller *et al.* (2005a) based their estimate on a combination of data from continental flooding (Bond, 1979; Harrison, 1990; Sahagian *et al.*, 1996; Fig. 12) that showed a range of ~80–150 m and other backstripping estimates of about +120 m for a Late Cretaceous peak (Watts & Steckler, 1979). Watts & Thorne (1984) revised the Watts & Steckler (1979) backstripped results in a forward modelling study of East Coast United States, and Scotian continental shelves. Their curve is quite consistent with ours, although it is slightly higher in the Coniacian, Turonian and Campanian (Fig. 12). It must be noted that both studies were carried out in the same general region, although the data sets used in the two studies are entirely independent and the Scotian margin sites used in their study are located over 1000 miles north of the New Jersey locations used in both studies. This certainly suggests that we have at least obtained a regional sea-level curve. Bond (1979) combined the area of continents flooded with continental hypsometry to obtain estimates of eustatic change and continental epeirogeny. His results have large error ranges, but are generally consistent with our results (Fig. 12).

Our results stand in sharp contrast with the long-term estimates of 250 m of Exxon Production Research Company (EPR; Vail and Mitchum, 1977; Haq *et al.*, 1987;

Fig. 12). Haq *et al.* (1987) scaled their long-term sea-level estimates to eustatic estimates based on spreading rate changes through time (Kominz, 1984, best estimate curve in Fig. 12). The Kominz (1984) results (230 m of long-term fall since 80 Ma) can be reconciled with the lower (100–150 m long-term fall) results if the spreading rates during the Cretaceous Quiet Zone were lower. In fact, Kominz (1984) showed that the full uncertainty in spreading rates and the effect of ocean ridge volume through time could have resulted in a sea-level range of 46–420 m above present in Late Cretaceous (80 Ma). This error range was dominated by uncertainties in the duration of the Cretaceous quiet zone. The lowest estimates of Kominz (1984) are entirely consistent with our sea-level estimates (Kominz (1984) Bio time scale, Fig. 12). Thus, if the Haq *et al.* (1987) curve were scaled to 145 m at 80 Ma, the global sequence stratigraphic curve would be much closer to our new sea-level curve.

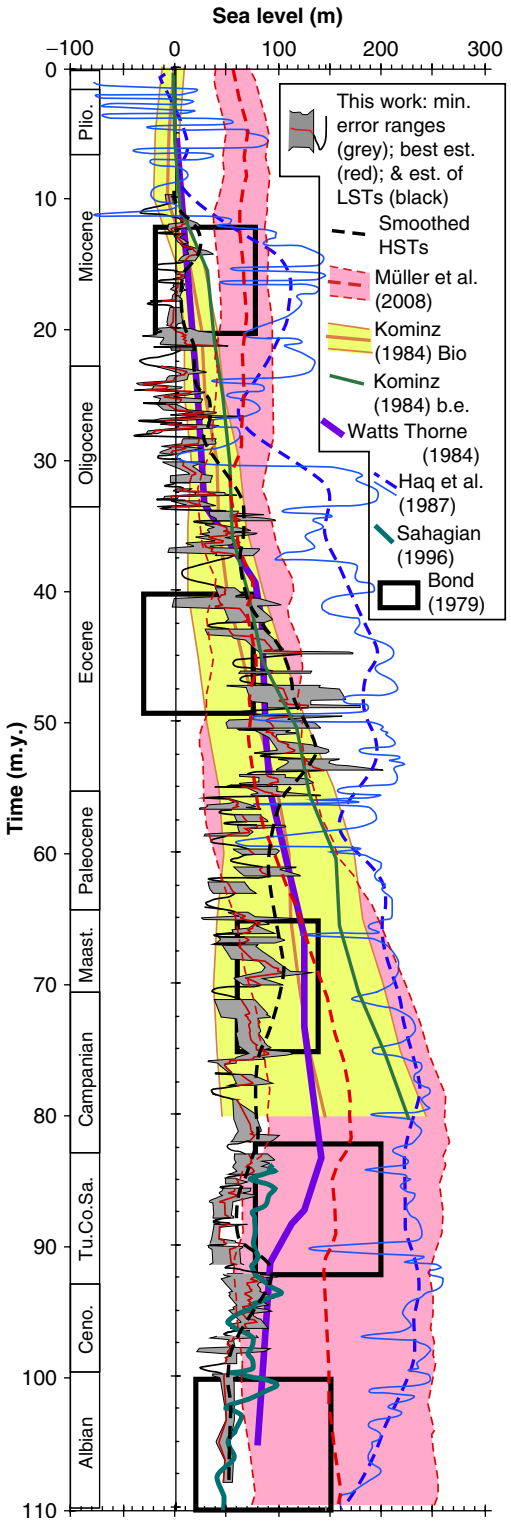

Müller *et al.* (2008) have calculated the effect of spreading rates, oceanic plateau emplacement, sedimentation, and ocean area change on ocean volume and, thus, sea level. Their results, which are calculated assuming an ice-free earth, require a long-term eustatic fall since the Late Cretaceous (80 Ma) of 90–260 m (Fig. 12). This result overlaps with the estimates of Bond (1979). The slightly lower ranges obtained from hyposometry may be fully reconciled with the ocean volume results of Müller *et al.* (2008) if continents are considered as subdivided into smaller units in recognition that epeirogenic uplift and subsidence may be regional (e.g. Spasojević *et al.*, 2008). In particular, a long-term epierogenic fall of the east coast of North America is required in order to reconcile our new regional sea-level curve with the Müller *et al.* (2008) eustatic curve in the Late Cretaceous (Fig. 12). A number of authors, including Conrad *et al.* (2004), Spasojevic *et al.* (2008) and Müller *et al.*, (2008) suggest that mantle dynamics caused the eastern portion of North America to subside as it overrode the subducted Farallon Plate. Because both the continent and sea level were subsiding at the same time, it would be impossible for backstripping to distinguish this long-term epeirogenic signal (Müller *et al.*, 2008).

Müller *et al.*, (2008) generated several models for the impact of the Farallon Plate on the long-term subsidence of

Fig. 12. Comparison of our new sea-level estimates to those derived using different methods. Kominz (1984) analysed the effect of sea floor spreading on ridge volumes and, thus, eustasy. Here the range of sea level, assuming minimum spreading rates (Bio) for the Cretaceous quiet period, and only the mean, best estimate results (b.e.) are plotted. Müller *et al.* (2008) has updated these curves by analysing ocean volume change including the effect of ridge volume, sediment volume, large igneous province emplacement, and the changing area of the oceans. Ice is not included in their results, which are plotted assuming an ice free world (54 m above today's sea level). Bond (1979) studied global continental flooding history and estimated a range of possible sea level for broad periods of time. Sahagian *et al.* (1993) carried out a detailed analysis of Cretaceous and older sea level on the stable Russian Platform. Watts & Thorne (1984) combined backstripping and forward modelling of the Atlantic coastal stratigraphy to derive their sea level estimates. Haq *et al* (1987) performed a sequence stratigraphic analysis of a global database and calibrated their curve to the best-estimate values of Kominz (1984) of 230 m at 80 Ma (b.e. curve). A smoothed version of our sea level curve was generated by connecting highstands and is comparable to the smoothed Haq *et al.* (1987) curve. (Plio., Pliocene; Ceno., Cenomanian; Tu.Co.Sa, combined Turonian, Coniacian and Santonian; Maast., Maastrichtian).

New Jersey. The magnitudes of the effect of dynamic topography generated by Müller *et al.* (2008) are consistent with those of Spasojevic *et al.* (2008) and Conrad *et al.* (2004). We use the modified backwards advection model of Müller *et al.*, (2008) in which the impact of mantle dynamics on New Jersey was based on mantle tomography from Ritsema *et al.* (2004) to correct our long-term curve for the subsidence due to mantle-derived dynamic topography (curve labelled 'This work – slab' in Fig. 13). If the lowstands were dominated by ice melting and re-growth they are not included in the long-term ocean-volume derived sea-level curve of Müller *et al.* (2008). Thus, we generate a long-term curve by connecting and smoothing highstands (Fig. 12). It is interesting to note that our uncorrected long-term curve is relatively consistent with the Müller *et al.*, (2008) eustatic curve in the middle Eocene and younger, if most of the world's ice is assumed to have accumulated between the late Eocene and the Pliocene (Fig. 13). However, our long-term curve is increasingly low beginning in the early Palaeocene and falls below the Müller *et al.*, (2008) low error limit in the Campanian. This is essentially the time when the slab-corrected curve becomes consistent with the Müller *et al.*, (2008) ridge volume curve. Thus, reconciling our new sea-level results from New Jersey with the ridge volume curve requires either: (1) a revised, earlier timing, of the epeirogenic impact of the Farallon slab on New Jersey; (2) an unrecognized tectonic reduction in the ocean volume (resulting in sea-level rise) throughout the Palaeocene and Eocene; or (3) an unrecognized additional tectonic effect in New Jersey that caused New Jersey to be low, relative to sea level from the Palaeocene through the middle Eocene (Fig. 13).

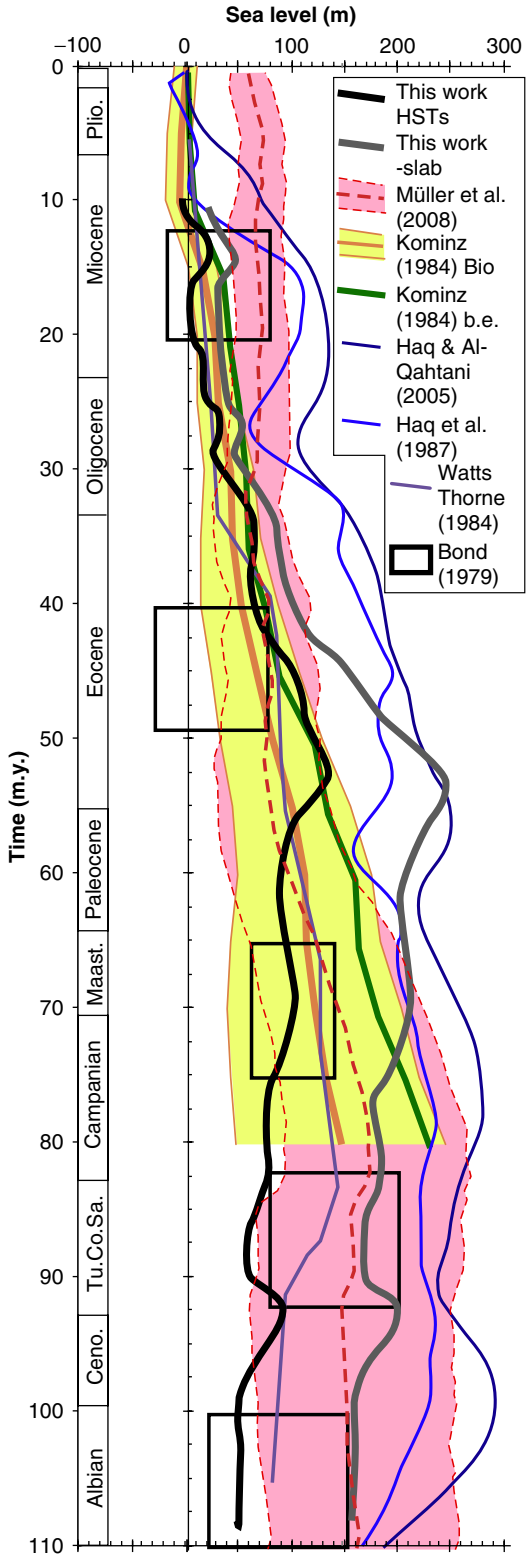

CONCLUSIONS

The generation of a sea-level curve from onshore stratigraphic data includes considerable uncertainty. The long-term trends (10^7 yr) are particularly dependent on the choice of thermal parameters and timing of the passive margin subsidence. Short-term errors (0.5–3.0 m.y. sequences) arise due to uncertainties in age and water depth as well as 2D loading effects. For the most part, *R*2 results from 11 coreholes are internally consistent and, as such, support the assumption of a sea level dominated signal. Rapid, large sea-level changes in the Late Cretaceous that correlate with unconformities in New Zealand are consistent with the presence of moderate ice sheets at that time. Our long-term sea-level curve is below that required by ocean volume calculations before 55 Ma. Current models

Fig. 13. Attempt to reconcile our long-term curve (This work HSTs) with recent calculation of sea level change due to changing ocean volume in an ice-free world (Müller *et al.*, 2008). The curve labelled 'This work – slab' adds the mantle dynamics due to the New Jersey coastal plain region overriding the subducted Farallon Plate as modelled by Müller *et al.*, (2008) to our long-term curve (This work HSTs). Kominz (1984) Bio and best estimate (b.e.) sea-level estimates are compared with the new Müller *et al.* (2008) estimates. For completeness both the smoothed Haq *et al.* (1987) and Haq & Al-Qahtani (2005) sequence stratigraphic sea-level curves are plotted as well as the Bond (1979) and Watts & Thorne (1984) sea level estimates. (See text for discussion. Ceno., Cenomanian; Tu.Co.Sa, combined Turonian, Coniacian and Santonian; Maast., Maastrichtian; Plio., Pliocene).

for mantle-generated dynamic topography in New Jersey resolve the long-term differences but are incompatible with the early Eocene sea-level maximum observed in our data set. Confirmation of the details and resolution of the inconsistencies await results from other margins and improved geodynamic modeling.

ACKNOWLEDGEMENTS

We thank the USGS ERMT drillers for obtaining cores from 11 of the onshore sites, Longyear/DOSECC for drilling Bass River, P. McLaughlin for obtaining logs at numerous sites, and P. McLaughlin and other members and collaborators of the coastal plain drilling project for data and discussions. We thank Craig Fulthorpe, Luc Lavier, Robert Sheridan and Steve Pekar for their careful reviews of the manuscript. Supported by NSF EAR037101 and NSF EAR981425, (Kominz), the New Jersey Geological Survey, NSF EAR99-09179, NSF/OCE/ODP OCE0623883 and EAR03-017112 (Miller).

REFERENCES

Benson, R.N. (2003) Age estimates of the seaward-dipping volcanic wedge, earliest oceanic crust, and earliest drift-stage sediments along the North American Atlantic. In: *The Central Atlantic Magmatic Province; insights from fragments of Pangea, Geophysical Monograph* (Ed. by W.E. Hames, J.G. McHone, P.R. Renne & C. Ruppel). **Vol. 136**, pp. 61–75. American Geophysical Union, Washington, DC, USA.

Bond, G.C. (1979) Evidence for some uplifts of large magnitude in continental platforms. *Tectonophysics*, **61**, 285–305.

Bond, G.C., Kominz, M.A. & Grotzinger, J.P. (1988) Cambro-Ordovician eustasy: evidence from geophysical modeling of subsidence in Cordilleran and Appalachian passive margins. In: *New Perspectives in Basin Analysis* (Ed. by Paola, C. & Kleinspehn, K.) pp. 129–161. Springer-Verlag, New York, NY.

Bond, G.C., Kominz, M.A., Steckler, M.S. & Grotzinger, J.P. (1989) Role of thermal subsidence, flexure and eustasy in the evolution of early Paleozoic passive-margin carbonate platforms. In: *Controls on Carbonate Platform and Basin Development* (Ed. by P.D. Crevello, J.L. Wilson, J.F. Sarg & J.F. Read), *SEPM (Soc. Sediment. Geol.) Specl. Publ.*, **44**, 39–61.

Bornemann, A., Norris, R.D., Friedrich, O., Beckmann, B., Schouten, S., Damste, J.S., Vogel, J., Hofmann, P. & Wagner, T. (2008) Isotopic evidence for glaciation during the Cretaceous supergreenhouse. *Science*, **319**, 189–192.

Browning, J.V., Miller, K.G., McLaughlin, P.P., Kominz, M.A., Sugarman, P.J., Monteverde, D.H., Feigenson, M.D. & Hernandez, J.C. (2005) Quantification of the effects of eustasy, subsidence, and sediment supply on Miocene sequences, mid-Atlantic margin of the United States. *Geol. Soc. of Amer. Bull.*, **118**, 567–588.

Browning, J.V., Miller, K.G., Sugarman, P.J., Kominz, M.A., McLaughlin, P.P., Kulpecz, A. & Feigenson, M.D. (2008) A 100 million year record of sequences, facies and sea-level change from Ocean Drilling Program onshore coreholes, U.S. Mid-Atlantic coastal plain. *Basin Res*, **20**.

Burgess, P.M. & Gurnis, M. (1995) Mechanisms for the formation of cratonic stratigraphic sequences. *Earth Planet. Sci. Lett.*, **136**, 647–663.

Camoin, G.F, Montaggioni, L.F. & Braithwaite, (2004) Late glacial to post glacial sea levels in the western Indian Ocean. *Mar. Geol.*, **206**, 119–146.

Crampton, J.S., Schioler, P. & Roncaglia, L. (2006) Detection of Late Cretaceous eustatic signatures using quantitative biostratigraphy. *Geo. Soc. Am. Bull.*, **118**, 975–990.

Conrad, C., Lithgow-Bertelloni, C. & Louden, K.E. (2004) Iceland, the Farallon slab, and dynamic topography of the North Atlantic. *Geology*, **32**, 177–180.

Divins, D.L. (2006) Total Sediment Thickness of the World's Oceans and Marginal Seas. http://www.ngdc.noaa.gov/mgg/sedthick/sedthick.html

Fairbanks, R.G. & Matthews, R.K. (1978) The marine oxygen isotope record in Pleistocene coral, Barbados, West Indies. *Quatern. Res.*, **10**, 181–196.

Fulthorpe, C.S. & Austin, J.A. Jr (1998) The anatomy of rapid margin progradation: three dimensional geometries of Miocene clinoforms, New Jersey margins. *Am. Assoc. Petrol. Geol. Bull.*, **82**, 251–273.

Greenlee, S.M. & Moore, T.C. (1988) Recognition and interpretation of depositional sequences and calculation of sea level changes from stratigraphic data-offshore New Jersey and Alabama Tertiary. In: *Sea Level Changes: An Integrated Approach* (Ed. by C.K. Wilgus, B.S. Hastings, C.G.St.C. Kendall, H.W. Posamentier, C.A. Ross & J.C. Van Wagoner), *Spec. Publ. Soc. Econ. Paleontol. Mineral*. **42**, 329–353.

Haq, B.U. & Al-Qahtani, A.M. (2005) Phanerozoic cycles of sea-level change on the Arabian Platform. *GeoArabia (Manama)*, **10**, 127–160.

Haq, B.U., Hardenbol, J. & Vail, P.R. (1987) Chronology of fluctuating sea levels since the Triassic (250 million years ago to present). *Science*, **235**, 1156–1167.

Harrison, C.G.A. (1990) Long-term eustasy and epeirogeny in continents. In: *Studies in Geophysics* (Ed. by R.R. Revelle, T.P. Barnett, E.J. Barron, A.L. Bloom, N. Christie-Blick, C.G.A. Harrison, W.W. Hay, R.K. Matthews, M.F. Meier, W.H. Munk, W.R. Peltier, D. Roemmich, W. Sturges, E.T. Sundquist, K.R. Thompson & S.L. Thompson), pp. 141–158. National Academic Press, Washington, DC, USA.

Hayden, T.G., Kominz, M.A., Powars, D.S., Edwards, L.E., Miller, K.G., Browning, J.V. & Kulpecz, A.A. (2008) Impact effects and regional tectonic insights: Backstripping the Chesapeake Bay Impact Structure. *Geology*, **36**, 327–330.

Huismans, R.S., Podladchikov, Y.Y. & Cloetingh, S. (2001) Dynamic modeling of the transition from passive to active rifting, application to the Pannonian basin. *Tectonics*, **20**, 1021–1039.

John, C.M., Karner, G.D. & Mutti, M. (2004) $\delta^{18}O$ and Marion Plateau backstripping: combining two approaches to constrain late middle Miocene eustatic amplitude. *Geology*, **32**, 829–832.

Kominz, M.A. (1984) Oceanic ridge volumes and sea level change – an error analysis. In: *Interregional Unconformities and Hydrocarbon Accumulation* (Ed. by J. Schlee), *Am. Assoc. Petrol. Geol. Memoir,* **36**, 109–127.

Kominz, M.A. & Pekar, S.F. (2001) Oligocene eustasy from two-dimensional sequence stratigraphic backstripping. *Geol. Soc. Am. Bull.*, **113**, 291–304.

Kominz, M.A. & Scotese, C.R. (2005) Thermal Cooling of Ocean Lithosphere – New Data – New Insights. *Am. Geophys. Union, Abstr.*, **6**, 259.

Larson, R.L. (1991) Geological consequences of superplumes. *Geology*, **19**, 963–966.

Lu, H., Fulthorpe, C.S., Mann, P. & Kominz, M.A. (2005) Miocene-Recent tectonic and climatic controls on sediment supply and sequence stratigraphy: canterbury basin, New Zealand. *Basin Res.*, **17**, 311–328.

McKenzie, D. (1978) Some remarks on the development of sedimentary basins. *Earth Planet. Sci. Lett.*, **40**, 25–32.

Miall, A.D. (1992) The Exxon global cycle chart: an event for every occasion? *Geology*, **20**, 787–780.

Miller, K.G., Barrera, E., Olsson, R.K., Sugarman, P.J. & Savin, S.M. (1999a) Does ice drive early Maastrichtian eustasy? Global $\delta^{18}O$ and New Jersey sequences. *Geology*, **27**, 783–786.

Miller, K.G., Browning, J.V. & Sugarman, P.J., *et al.* (2003) 174AX leg summary sequences, sea level, tectonics, and aquifer resources: coastal plain drilling. In: *Proceedings of Ocean Drilling Program, Initial Reports, 174AX (Suppl.)* (Ed. by K.G. Miller, P.J. Sugarman & J.V. Browning, *et al.*) pp. 1–40. Ocean Drilling Program, College Station, TX.

Miller, K.G., Kominz, M.A., Browning, J.V., Wright, J.D., Mountain, G.S., Katz, M.E., Sugarman, P.J., Cramer, B.S., Christie-Blick, N. & Pekar, S.F. (2005a) The Phanerozoic record of global sea-level change. *Science*, **310**, 1293–1298.

Miller, K.G., Liu, C., Browning, J.V., Pekar, S., Sugarman, P.J., Van Fossen, M.C., Mullikin, L., Queen, D., Feigenson, M.D., Aubry, M.-P., Burckle, L.D., Powars, D. & Heibel, T. (1996) Cape May site report. *Proc. Ocean Drill. Program, Init. Repts.*, **150X**, 5–28.

Miller, K.G., Sugarman, P.J., Browning, J.V., Cramer, B.S., Olsson, R.K., Metzger, K., Monteverde, D., Pekar, S.F., Reilly, T.R., Skinner, E., Uptegrove, J., de Romero, L., Aubry, M-.P., Bukry, Queen, D., Mullikin, L., Muller, L. & Stewart, M. Ancora Site Report, Proceedings of the ODP, Initial Reports, 174AX: (suppl.) College Station, TX (Ocean Drilling Program), 1999b.

Miller, K.G., Sugarman, P.J., Browning, J.V., Kominz, M.A., Olsson, R.K., Feigenson, M.D. & Hernandez, J.C. (2004) Upper cretaceous sequences and sea-level history, New Jersey coastal plain. *Geol. Soc. Am. Bull.*, **116**, 368–393.

Miller, K.G., Sugarman, P.J., Browning, J.V., Olsson, R.K., Pekar, S.F., Reilly, T.R., Cramer, B.S., Aubry, M.-.P., Lawrence, R.P., Curran, J., Stewart, M., Metzger, J.M., Uptegrove, J., Bukry, D., Burckle, L.H., Wright, J.D., Feigenson, M.D., Brenner, G.J. & Dalton, R.F. (1998) Bass River Site Report, Proceedings of the ODP, Initial Reports, 174AX*:* College Station, TX (Ocean Drilling Program), 39pp..

Miller, K.G., Wright, J.D. & Browning, J.V. (2005b) Visions of ice sheets in a greenhouse world. *Marine Geol.*, **217**, pp. 215–231.

Müller, R.D., Roest, W.R., Royer, J.-Y., Gahagan, L.M. & Sclater, J.G. (1997) A digital age map of the ocean floor. SIO Reference Series 93–30, Scripps Institution of Oceanography. http://www.geosci.usyd.edu.au/research/marinegeophysics/Resprojects/A gegrid/Images/globe.ind.gif

Müller, D., Sdrolias, M., Gaina, C., Steinberger, B. & Heine, C. (2008) Long-term sea level fluctuations driven by ocean basin dynamics. *Science*, **319**, 1357–1362.

Parsons, B. & Sclater, J.G. (1977) An analysis of the variation of ocean floor bathymetry and heat flow with age. *J. Geophys. Res.*, **82**, 803–827.

Pekar, S.F., Christie-Blick, N., Kominz, M.A. & Miller, K.G. (2002) Calibration between glacial eustasy and oxygen isotopic data for the early icehouse world of the Oligocene. *Geology*, **30**, 903–906.

Pekar, SF., Christie-Blick, N., Miller, K.G. & Kominz, M.A. (2003) Quantitative constraints on the origin of stratigraphic architecture at passive continental margins: Oligocene sedimentation in New Jersey, USA. *J. Sediment. Res.*, **73**, 227–245.

Pekar, S.F., Miller, K.G. & Kominz, M.A. (2000) Reconstructing the stratal geometry of latest Eocene to Oligocene sequences in New Jersey: resolving a patchwork distribution into a clear pattern of progradation. *Sediment. Geol.*, **134**, 93–109.

Pitman, W.C. & Golovchenko, X. (1988) Sea-level changes and their effect on the stratigraphy of Atlantic-type margins. In: *The Atlantic Continental Margin; US, The Geology of North America* (Ed. by R.E. Sheridan & J.A. Grow). **I-2** pp. 429–436. Geological Society of America, Boulder, CO, USA.

Posamentier, H.W., Jervey, M.T. & Vail, P.R. (1988) Eustatic controls on clastic deposition I – Conceptual framework. In: *Sea Level Changes: An Integrated Approach* (Ed. by C.K. Wilgus, B.S. Hastings, C.G.St.C. Kendall, H.W. Posamentier, C.A. Ross & J.C. Van Wagoner), *Spec. Publ., Soc. Econ. Paleontol. Mineral.*, **42**, 109–124.

Ritsema, J., van Heijst, H.J. & Woodhouse, J.H. (2004) Global transition zone tomography. *J. Geophys. Res.*, **109**, 2302–2316.

Sahagian, D., Pinous, O., Olferiev, A. & Zakharov, V. (1996) Eustatic curve for the Middle Jurassic–Cretaceous based on Russian platform and Siberian stratigraphy: zonal resolution. *AAPG Bull.*, **80**, 1433–1458.

Sheridan, R.E., Olsson, R.K. & Miller, J.J. (1991) Seismic reflection and gravity study of proposed Taconic suture under the New Jersey Coastal Plain: implications for continental growth. *Geol. Soc. Am. Bull.*, **103**, 402–414.

Smith, W.H.F. & Sandwell, D.T. (1997) Global seafloor topography from satellite altimetry and ship depth soundings, Science, **277**, p. 1957–1962. http://topex.ucsd.edu/cgi-bin/get.data.cgi (University of California San Diego).

Spasojevic, S., Liu, L., Gurnis, M. & Muller, R.D. (2008) The case for dynamic subsidence of the United States east coast over the Cenozoic. *Geophys. Res. Lett.*, in review.

Steckler, M.S., Mountain, G.S., Miller, K.G. & Christie-Blick, N. (1999) Reconstructing the geometry of Tertiary sequences on the New Jersey passive margin by 2-D backstripping: the interplay of sedimentation, eustasy and climate. *Marine Geol.*, **154**, 399–420.

Steckler, M.S. & Watts, A.B. (1978) Subsidence of the Atlantic-type continental margins of New York. *Earth Planet. Sci. Lett.*, **41**, 1–13.

Steckler, M.S., Watts, A.B. & Thorne, J.A. (1988) Subsidence and basin modeling at the U.S. Atlantic passive margin. In: *The Atlantic Continental Margin; U.S., The Geology of North America* (Ed. by R.E. Sheridan & J.A. Grow), **I-2** pp. 399–416. Geological Society of America, Boulder, CO, USA.

Stein, C.A. & Stein, S. (1992) A model for the global variation in oceanic depth and heat flow with lithospheric age. *Nature*, **359**, 123–129.

Sugarman, P.J., Miller, K.G., Browning, J.V., Kulpecz, A.A. & McLaughlin, P.P. (2005) Hydrostratigraphy of the New Jersey Coastal Plain: sequences and facies predict continuity of aquifers and confining units. *Stratigraphy*, **2**, 259–275.

Vail, P.R. & Mitchum, R.M. Jr (1977) Seismic stratigraphy and global changes of sea level, Part 1: overview. In: *Seismic Stratigraphy – Applications to Hydrocarbon Exploration* (Ed. by C.E. Payton), *Am. Assoc. Petrol. Geol. Memoir.*, **26**, 51–52.

Van Sickel, W.A., Kominz, M.A, Miller, K.G. & Browning, J.V. (2004) Late cretaceous and cenozoic sea-level estimates backstripping analysis of borehole data, Onshore New Jersey. *Basin Res.*, **16**, 451–465.

Watts, A.B. & Thorne, J. (1984) Tectonics, global changes in sea level and their relationship to the stratigraphical sequences at the US Atlantic continental margin. *Mar. Petrol. Geol.*, **1**, 319–321.

Watts, A.B. & Steckler, M.S. (1979) Subsidence and eustasy at the continental margin of eastern North America. In: *Deep Drilling Results in the Atlantic Ocean: Continental Margins and Paleoenvironments* (Ed. by M. Talwani, W.W. Hay & W.B.F. Ryan), *AGU Maurice Ewing ser.,* **3**, 218–234.

White, R. & McKenzie, D. (1989) Magmatism at rift zones; the generation of volcanic continental margins and flood basalts. *J. Geophys. Res.*, **94**, 7685–7729.

Manuscript received 20 June 2007; Manuscript accepted 10 February 2008.

Supplementary material

The following material is available for this article online:

Table S1. Minimum, Maximum and Best Estimate Sea Level Estimates, from Coastal Plain Coreholes, New Jersey and Delaware.

Table S2. Long-term Sea Level from this work and Long-term Sea-Level Corrected for Dynamic Response of Mantle to Overriding the Farallon Plate (from Müller *et al.*, 2008).

This material is available as part of the online article from: http://www.blackwell-synergy.com/doi/abs/10.1111/j.1365-2117.2008.00354.x (This link will take you to the article abstract).

Please note: Blackwell Publishing are not responsible for the content or functionality of any supplementary materials supplied by the authors. Any queries (other than missing material) should be directed to the corresponding author for the article.

